PHYSICAL CHARACTERIZATION OF CARBONACEOUS PRODUCTS FROM FIRE AND FIRE RETARDANTS: ASSESSMENT OF THE IMPACT ON FIRE PERFORMANCE

Gizem Okyay, Anil Naik, Pauline Tranchard, Séverine Bellayer, Maude Jimenez, Fabienne Samyn, Serge Bourbigot

HAL Id: hal-01879764

https://hal.univ-lille.fr/hal-01879764v1

Submitted on 24 Sep 2018

PHYSICAL CHARACTERIZATION OF CARBONACEOUS PRODUCTS FROM FIRE AND FIRE RETARDANTS: ASSESSMENT OF THE IMPACT ON FIRE PERFORMANCE

Gizem Okyay, Anil Naik, Pauline Tranchard, Séverine Bellayer, Maude Jimenez, Fabienne Samyn and Serge Bourbigot*

R₂Fire group, UMET-ISP, CNRS UMR 8207, ENSCL, University of Lille, Villeneuve d'Ascq, France

INTRODUCTION

In fire research and safety, it is crucial to understand the kinetics and processes behind the fire phenomenon and the response of materials exposed to it. One should examine the two components of fire: the flame itself and the materials burning in order to assess the fire performance. Those two components can be examined separately or together, depending on the topic and the research interests such as fire spread[1], chemical and physical kinetics[2,3], etc.

Burning of materials, flame retarded or not, leads to the release of heat and combustion products and in particular, carbonaceous products such as soot, ash and char in gaseous and condensed phases. In fire research, it is crucial to study the interactions of this evolved heat with its surroundings, which can become complex due to the kinetics and all modes of heat transfer involved. The response of material to heat is a function of its properties, such as the chemical composition, thermal decomposition, emissivity, morphology, etc. Those properties are eventually time dependent due to the evolution of chemistry and structure throughout burning. Hence, a way to investigate the fire performance of a material is to quantify the above mentioned properties as a function of time when possible.

The objective of this research is to improve the overall understanding of our fire testing and modeling tools, in order to propose better solutions to make fire barrier materials. Here, the morphology and the thermal conductivity are chosen as variables/parameters to examine fire behavior and fire performance. The studied materials and the testing conditions, further detailed in the materials and methods section, have been chosen based on the accumulated experiences and the know-hows of our team. The focus of this study is on the morphology of carbonaceous products issued from burning and it was decided to consider separately the phenomena occurring in the flame and in the material itself.

For the fire tests where radiation dominates (e.g. cone calorimeter test), the emphasis is given on the gaseous phase and flame (i.e. its soot particulate media) because soot is known to be the main heat source and sink of flame emissions[4]. It is also a pollutant and affects the toxicity. The particulate media is extracted and analyzed from the burning of gaseous decompositions of EVA (Ethylene-Vinyl Acetate) and its fire retarded formulation EVA/ATH (EVA loaded with ATH, aluminum trihydroxide mineral filler).

_____

* Correspondence: serge.bourbigot@ensc-lille.fr

For the fire tests where convection and conduction dominate (e.g. furnace tests), the emphasis is given to

the condensed phase. Intumescent coatings, and more precisely intumescent chars, which act as heat barrier between the flame and the substrate, is investigated. Knowing that their thermal conductivity plays an important role[5], their expansion pattern and thermal conductivity of the expanded char versus temperature are of interest.

MATERIALS AND METHODS

Study of soot particles in gaseous phase burning

According to state of the art[6,7], thermal degradation of polymeric materials can produce combustible hydrocarbon gases such as methane, propane, ethane, ethylene, etc. Those gases are known to produce nano and micron sized black carbon soot upon burning. Hence, it is possible to examine the decomposition history by observing those carbonaceous particles/residues during fire tests.

EVA copolymer was selected for the study of particulate media because it is a well-known material in fire research and the aim is also to complement the existing studies of our team[6,7,8,9]. Both EVA and EVA/ATH samples were tested, because the effect of flame retardant system on the emitted particulate media should play a significant role. The particulate media was formerly tested by filtering exhaust gas and by low pressure impactor techniques. The chemical composition of the gas phase was investigated by thermogravimetric analysis (TGA)/Fourier Transform Infrared (FTIR) and mass loss cone calorimeter (MLCC) also coupled to FTIR methods.
In this study, an innovative approach is being developed, never used by now in flame retardancy research: the soot particles and agglomerates morphology are studied directly from microscopy imaging with subsequent image processing. The aim is to retrieve information on the particle size (i.e. primary particle size, which is not be confused with the agglomerate size) to observe visually the agglomeration phenomenon and to visualize the time-dependent formation history of particles from our reference polymeric materials.

- Tested specimens:

Specimens used are: pure EVA (containing 28 wt % of vinyl acetate) and EVA/ATH (containing 65 wt% ± 5 wt%). Samples of size 10x10x0.3 cm^3 were prepared by extrusion and by molding for MLCC test, using the materials and methods detailed and verified in former studies[6].

- Fire testing:

The reaction to fire of materials were performed on a mass loss cone calorimeter (MLCC) from Fire Testing Technology (FTT) according to standards ISO 13927 or ASTM E906. The external heat source is only radiative in MLCC; hence the combustion products are intrinsic to the burning of the material, contrary to experiments where the material is subjected to an external flame. For example, in UL94 and UL1709 tests, it is highly probable to collect particles and burnt gases from the external heat source and not only from the material itself. MLCC tests were performed at mild fire scenario of 35 kW/m^2 incident radiative heat flux, with 25 mm separation distance between the heat source and sample surface. At least two MLCC experiments were performed on each material in order to ensure repeatability within the error margins of +/- 10%.

- Particle sampling:

Soot was sampled by using the particle deposition from flame, technique formerly applied and verified in combustion research[10]. The specimens were probed on Transmission Electron Microscopy (TEM) grids

(lacey and holey carbon film covered, square mesh copper grids, provided by Agar Scientific). The times of particle sampling were determined according to the characteristic times of the heat release rate (HRR) in MLCC experiments: just after the time to ignition, just after the maximum value of the peak of HRR, and at the end of test before flameout. In this study, only the latter two sampling times will be presented because they lead to highest amount of soot agglomerates.

- Microscopy:

Soot imaging was performed using Scanning Electron Microscopy (SEM) in transmission mode (SEM/STEM). STEM images were taken using a JEOL 7800 FEG LV scanning electron microscope at 30 kV and 7 mA, using a retractable bright and dark field SEM STEM detector completed with Deben Gen5 electronics and a 12 position TEM grid holder.

- Morphology analysis:

Numerical analyses were performed using the electron microscopy recordings, following the methodologies explained and verified in previous researches[11]. Particle counting and the size measurements were performed over more than 20 microscopy recordings for each material type. ImageJ[12] and its plugins were used for image processing and quantitative measurements.

Study of char from intumescent coatings

Former works on intumescent char structure focus on the expansion as a function temperature, on the possible synergies between ingredients of coatings[13] and on kinetics of degradation[14]. Nevertheless, the char morphology should be examined for further consideration, for example in numerical simulations and for better interpretation of thermal conductivity measurements[15].

In this paper, focus is given on the testing and analyses methods of the geometry of the expanded char. The repartition and size of bubbles/pores play an important role for fire properties of intumescent char[15], but it is difficult to integrate such information in modeling and simulation tools, either numerically or experimentally. Therefore, the aim of this study is to determine, if possible, a mathematical formulation of the inner structure with a perspective on its effect on thermal conductivity.

- Intumescent char specimens:

Two types of intumescent chars were examined: one obtained from a commercial epoxy based intumescent coating and the other from a silicon based intumescent coating developed in our lab and described elsewhere[16]. The coated steel plates were subjected to UL1709 fire testing to obtain expanded char specimens. The intact intumescent chars were then analyzed by X-ray tomography, and then cut for visual inspection.

- X-ray Tomography:

X-ray micro-computed tomography (μCT) was applied on chars collected from fires tests (UL1709). This is a non-intrusive technique to observe the inner morphology without structural damage. The tomography was performed using the micro-tomography setup (UltraTom from RX Solutions) at the ISIS4D X-ray μCT platform (Villeneuve d'Ascq, France)[17].

The tomography set-up consists of two X-ray tubes (micro and nano focus), a sliding and rotating stage holder, a flat panel detector (1920*1496 px – 127 µm/px – 0.2 to 60 frame/s), a linear detector (2560 px –

200 µm/px – 0.2 to 60 frame/s), a CCD camera (4000*2624 px – 11.8 µm/px – up to 3.4 frame/s) and an image intensifier.

The char samples were placed on styrofoam holders and then mounted on the rotating stage to minimize the signal noise due to the holder. The epoxy based char had to be placed with its steel plate, while the silicon based char was easily detached from its steel plate and placed on styrofoam directly. Samples were rotated by 360° with an angular step of 0.25°. The subsequent tomography volumes were reconstructed from 1440 projection images and visualized using X-Act (from RX Solutions): reconstructions have a resolution of 81µm/voxel in 3D space.

- Morphology analyses:

Image stacks of the inner structure were generated by slicing the reconstructed 3D volume. Those image stacks were re-processed to adjust gray signal levels to ensure the maximum visibility of carbon elements, noting that low atomic number elements interact only little with X-rays, hence tend to produce low gray levels in stack images[13]. Slice images were binarized for fractal analysis. ImageJ[12] software was used for the image processing. Quantitative analyses of mass density autocorrelations were performed using fractal analysis: Box-counting technique, previously applied on combustion soot[11], was re-written as C++/Matlab algorithms, and applied on µCT image slices of chars.

- Thermal conductivity measurements:

Thermal conductivity was measured from ambient to 500°C using a Transient Plane Source method (TPS2500S) from THERMOCONCEPT (Merignac, France). A thin hot disk sensor is placed between two pieces of sample acting both as heat generator and sample temperature gauge. An adequate sensor is placed between two 10 mm thick disk of 30 mm² diameter of the sample. To ensure a good contact between the sensor and the sample, the sensor was placed during manufacturing process between both sample disks. Then, the sample was degraded to get a thermally stable char. For each temperature, the measurements were performed as soon as the sample temperature was down to +/- 0.5°C of the desired temperature. The furnace was directly connected to a nitrogen flow and all experiments were carried out in an inert atmosphere to prevent oxidation of the sensor and of the char samples. The experiments were run as duplicated and were repeatable within 5-20% margin error.

RESULTS AND DISCUSSION

Particulate media in gaseous phase

Mass loss cone calorimeter experiments were performed on EVA and EVA/ATH. The resulting HRR curves are presented in Fig.1(a) and Fig.1(b) respectively: error margin of the experimental setup is +/- 10%. The probing time is less than or equal to one second. Hence, and as evidenced by the HRR curves, the effect of the soot probing during experiments is negligible. The soot sampling is repeated at the same specific times after ignition, on two different specimens: the results are similar, hence the repeatability of experiments is ensured. This is expected, because the thermal decomposition pathway of the specimens should remain constant throughout the same experimental conditions.
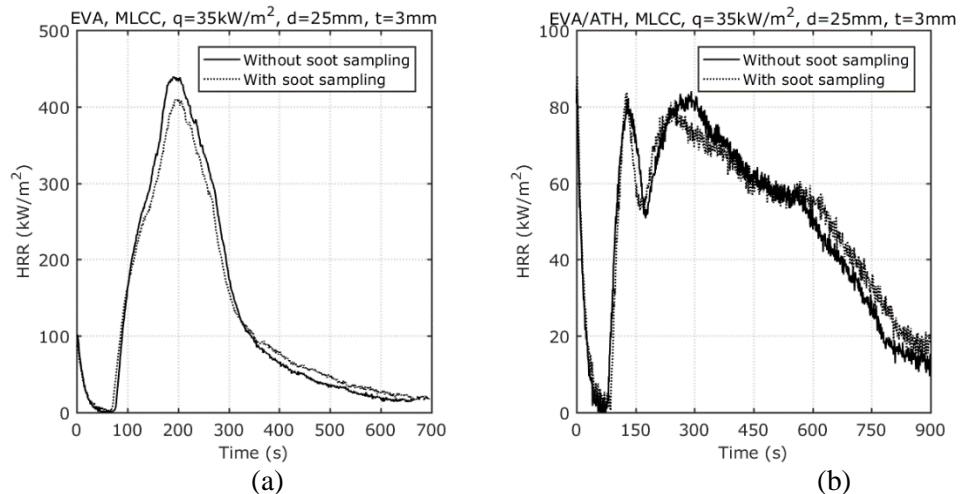
Figure 1. HRR curves from MLCC experiments on (a) EVA and (b) EVA/ATH

First qualitative observations on the extracted particles from burning EVA formulations are presented in Fig. 2. On Fig.2a, the soot dispersion on TEM grid from EVA is presented: variable sizes of particles and aggregates are observed. On Fig.2b, the soot dispersion on TEM grid from EVA/ATH is presented: tiny aggregates are observed, presumably with some residues of aluminum from ATH. The preliminary observations indicate a higher density of particles inside the gaseous volume for the non-flame retarded (FR) system.

In the FR system the soot emissions are somehow inhibited. This latter was expected because the incorporation of ATH reduces the release of flammable gases thanks to high loading (65 wt% ATH decreasing the polymer content) and to water release (dehydration of ATH), to decrease the system temperature (high endothermic effect due to the dehydration of ATH), hence leading to overall reduction of the formation kinetics of soot[6,18].
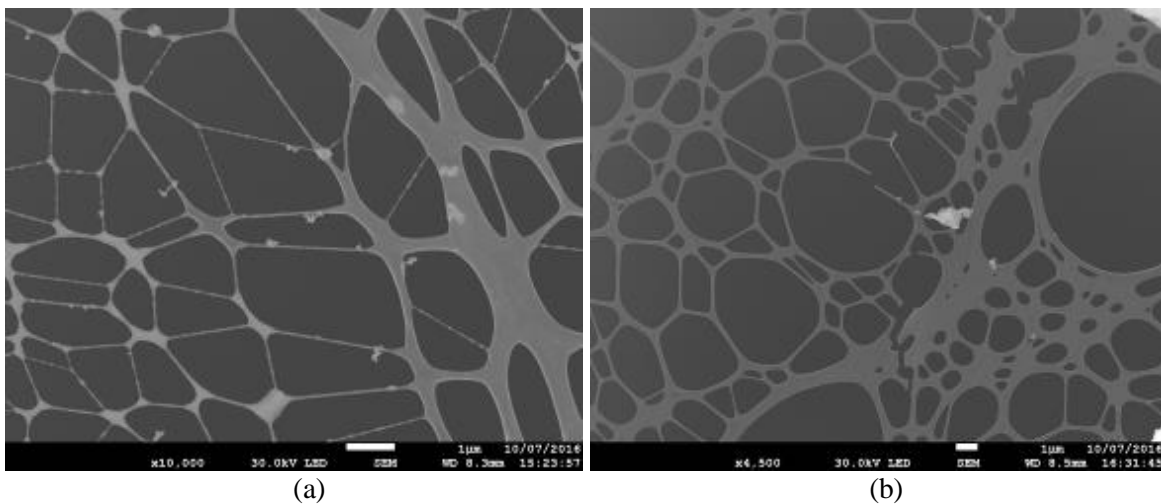

Figure 2. SEM/STEM images of particles collected from evolved gases of MLCC experiments of (a) EVA and (b) EVA/ATH, to make a qualitative comparison of density of particulate media.

In the next paragraphs, both EVA and EVA/ATH soot agglomerates are investigated separately.

- Investigation of soot from EVA as a neat polymer:

Images of soot extracted from EVA burning are presented in Fig.3a and Fig.3b.: they correspond to different probing times during MLCC test. The agglomeration pattern seems to be independent of probing time. As observed on Fig.3a, soot is in a coated form when extracted just after the peak of HRR. It is believed that some pieces of material are detached and melted on the soot substrate to form coated aggregates, presumably with some other decomposed material condensed on the agglomerates issued from the gaseous decomposition of EVA[6,17]. Aggregates are bare when extracted at the end of experiment as illustrated in Fig.3b.
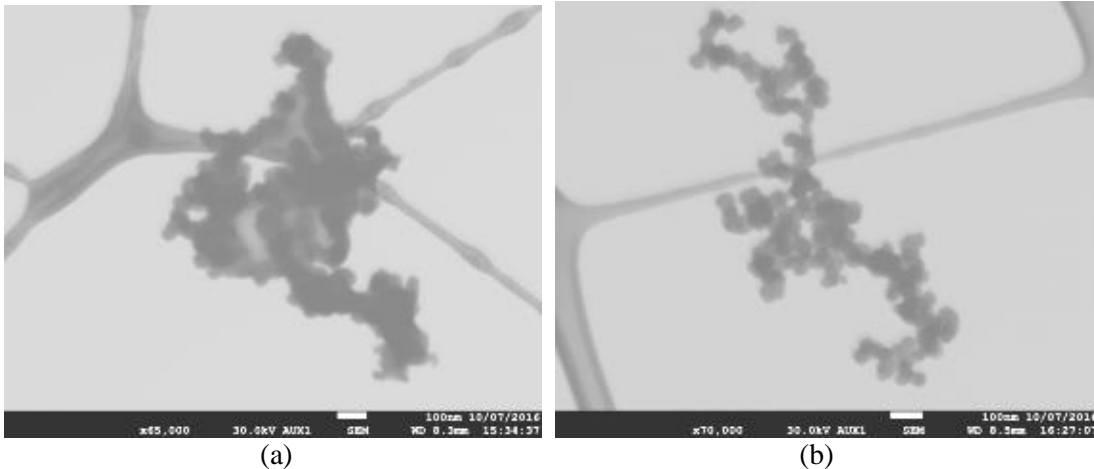

(a)   (b)

Figure 3. Example of SEM/STEM images of soot agglomerates collected (a) just after the peak of HRR and (b) before flameout from MLCC experiments of EVA.

The diameters of primary particles are measured on microscopy recordings in order to investigate the size distribution function. According to the probability density function of EVA soot, given in Fig.4, the particle size distribution is multimodal noting that the normal distribution (mean size of 29.5 nm; standard deviation of 11.6 nm) is plotted as a comparison to the real distribution. The modes are dependent on the type of hydrocarbons burning simultaneously.

Based on literature review on combustion soot[11]: small particle size (around 20-25 nm) is characteristic of methane combustion; medium particle size (around 30-35nm) is characteristic of ethylene and ethane combustion; larger particle sizes are generally issued from heavier hydrocarbon burning like propane, toluene, etc. It is believed that the highest peak in Fig.4 belongs to the burning of methane, whereas it is difficult to distinguish between ethane and ethylene peak. The existence of a third peak is novel compared to the results of smoke particles[18], and indicates traces of soot issued from heavier hydrocarbons and slower reactions. This will be further discussed in a separate paper, together with complementary chemical analyses on the gaseous phase and with potential dependencies on combustion kinetics.
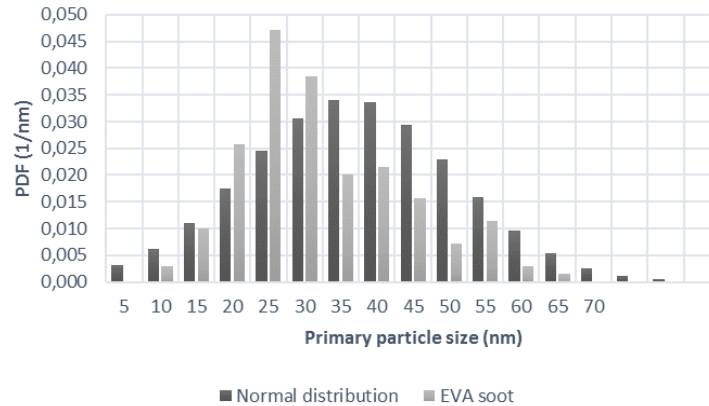
Figure 4. Particle size analysis for agglomerates from EVA burning.

- Investigation of soot from EVA/ATH as a FR system:

Images of soot extracted from EVA/ATH burning are presented in Fig.5. Soot samples probed just after the peak of HRR are coated with a thin layer, as observed in Fig.4a. The agglomeration pattern seems to remain the same according to the bare soot sample presented in Fig.4b. Those results are similar to those obtained for pure EVA.

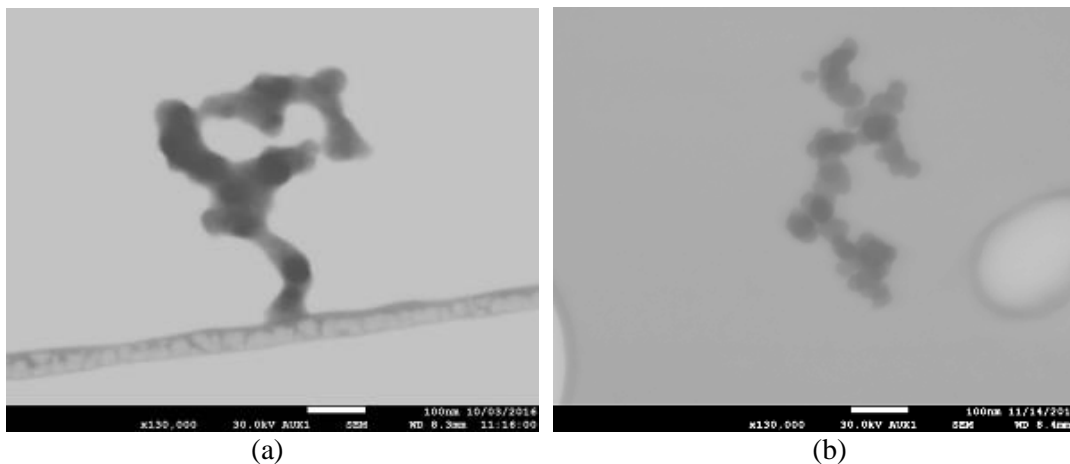(a)   (b)

Figure 5. Example of SEM/STEM images of soot agglomerates collected just after the peak of (a) HRR and (b) before flameout from MLCC experiments of EVA/ATH specimens.

According to the probability density function of EVA/ATH soot given in Fig.6, the particle size distribution is unimodal around 35-40 nm for EVA/ATH soot. The normal distribution (mean size of 34.4 nm; standard deviation of 8.9nm) is plotted as a comparison to the real multimodal distribution. The result is in accordance with the previous results on EVA/ATH decomposition where the propane release is favored with a mass density greater than the overall release of methane and ethane during controlled atmosphere MLCC tests[6]. Existence of lighter hydrocarbons can justify the skewness of the particle size distribution function.
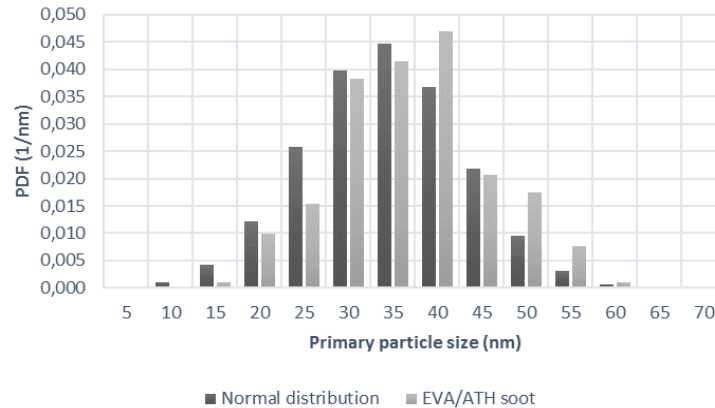
Figure 6. Particle size analysis for agglomerates from EVA/ATH burning.

To sum up, according to the observations on pure EVA and FR EVA/ATH, the volume density and polydispersity of particles is reduced in the flame retarded system. The mean particle size is however found to be larger for this FR EVA/ATH system and this leads to two hypotheses: the mass density of heavier hydrocarbons can be higher in the gaseous decomposition phase and the residence time of soot is longer following the slower reactions due to FR effect.

Some of the particle size measurements, both for EVA and EVA/ATH burning, have an uncertainty due to the coating of aggregates: the coating layer can impact the measurements by up to 5 nm to 10 nm depending on the image resolutions. Another source of error can be the usage of SEM/STEM, due to its lower precision compared to TEM.

The nanoscale morphology of particles cannot be observed in STEM. Nevertheless, the aggregation of primary particles can be observed with preliminary measurements on primary particle size. Also, the specimen is less susceptible to be damaged and polluted, with the usage of lower electron acceleration voltages. Therefore, the measurements are less affected by the deposition of a pollution layer and the restructuring of agglomerates, under the energy of the incident electron beam, justifying our study using SEM/STEM. Error margins (which are dependent on microscopy conditions and on user experience in image processing) will be investigated by future studies on sampling and imaging protocols.

Intumescent char

In the condensed phase, the focus is given to the structure of the expanded char. The final morphology of the expanded intumescent char of epoxy and silicon based coatings submitted to fire test are given in Fig.7(a) and Fig.7(b) respectively. The thickness of the epoxy based char is higher and less uniform compared to the silicon based char. The real life images are visually compared to the reconstructed numerical volumes from tomography illustrated in Fig.8.

(a)   (b)

Figure 7. Intumescent char formed from intumescent coatings on steel plates, with (a) epoxy based and (b) silicon based formulations, after UL1709 hydrocarbon fire test.

As it can be seen in Fig.7a and Fig.8a, some part of the information is lost for the epoxy based char, because the steel plate could not be detached without damaging the sample. The steel plate scattered the X-rays resulting in the noisy signals in tomography at the lower part of the char. Hence the quantitative image analyses were performed by suppressing this noisy region from the reconstructions of the X-ray µCT.
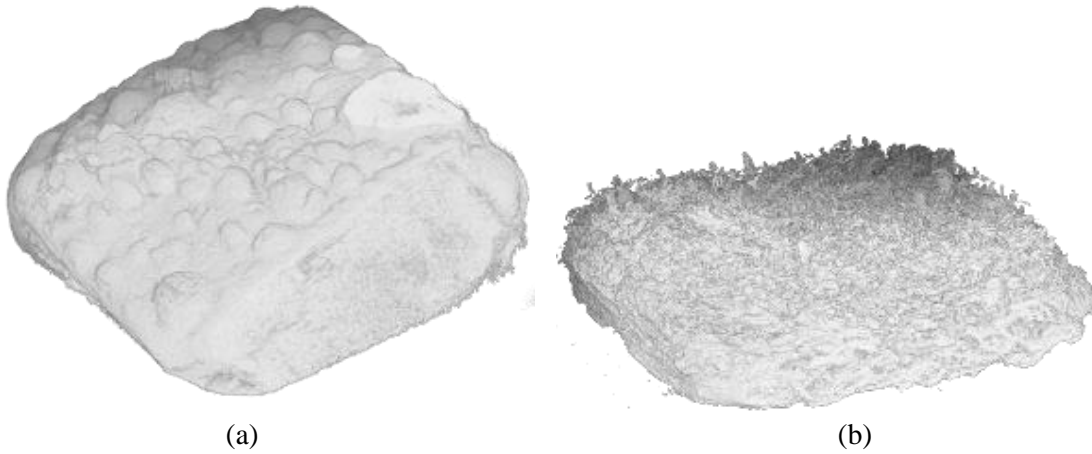

(a)   (b)

Figure 8. 3D geometries reconstructed from X-ray µCT of the (a) epoxy based char, (b) silicon based char.

In Fig. 9, the vertical slices were plotted after the X-ray µCT reconstruction. The epoxy based char in Fig.9a contains bubbles of different sizes with a non-uniform distribution. The silicon based char in Fig.9b contains more voids, more uniformly distributed in the vertical direction.

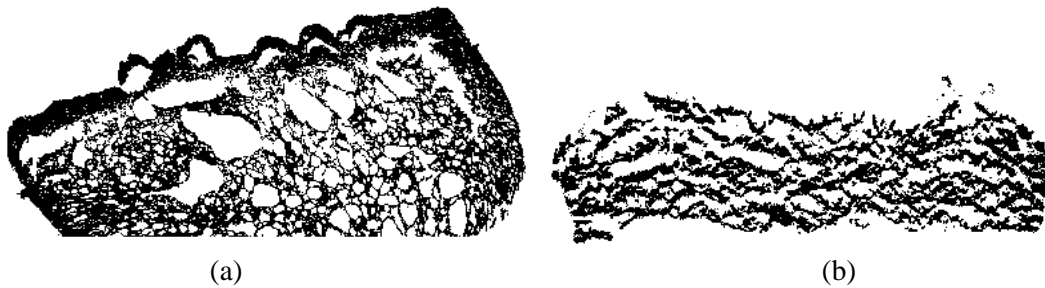(a)   (b)

Figure 9. Binarized slice images of the inner structures of (a) epoxy based char, (b) silicon based char.

Numerical analyses were then performed to investigate the possible existence of a density relationship.

-   Numerical analyses on morphology:

Box counting operation was performed in 2D space on tomography slice images of Fig.9 and plotted in Fig.10. The analysis was performed in macro and mesoscale (1 pixel = 81 microns). The computations were repeated for different vertical slices of the char to check any anisotropy inside the material. Starting from the outer vertical face of each char (visible side on the images of Fig.7), different slices were chosen at distances of 3 to 7 centimeters: The captions in Fig.10 are named accordingly and "5cm" corresponds to the middle vertical slice. As the analyses were performed in 2D space, the slope of the space-filling curve corresponds to the maximum slope of 2.

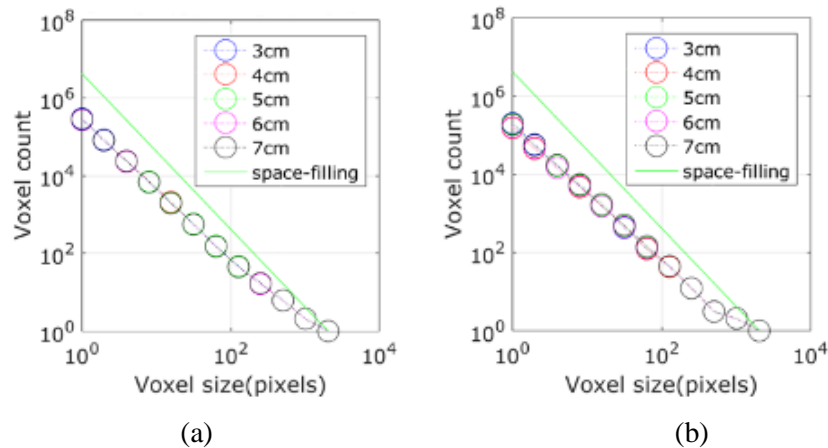(a)   (b)

Figure 10. The fractal analyses: (a) for epoxy based char, (b) for silicon based char.

The preliminary results indicate three main outcomes:

-   The fractal dimension is similar for both chars looking at the average slopes of the curves of Fig.10a and Fig.10b.

-   The distribution of void spaces, in each vertical slice, is more uniform for silicon based char. This is indicated by the uniformity of the slope of the log-log curves (except at the very macroscopic level). Indeed, the bubbly distribution of the epoxy based char is highly non-uniform from top to bottom, even with visual observations of Fig.10a. Hence, one can say that this mathematical description of morphology is consistent with observations.

-   When different vertical slices of the same material are compared, the distribution of void spaces is less uniform for silicon based char of Fig.10b. The analyses of different slices overlap for epoxy based char. For silicon based char, the values start to diverge from mesoscale (medium voxel size) to micro scale (small voxel size). This difference is due to different intumescence mechanisms of both formulations. The epoxy-based formulation is a conventional intumescent system involving charring reactions from the ingredients contained in the material. The silicone-based formulation is based on expandable graphite. The rapid sublimation of sulfuric acid inserted in the graphite platelets creates growing 'worms' forming the intumescent char. It will be commented in future works.

-   Experimental results on thermal conductivity:

Thermal conductivity of silicone/modifier and epoxy/modifier were measured from ambient temperature up to 500°C. For epoxy based char, it varies from 0.14 to 0.5 W/m.K depending on the temperature. For the silicon based char, the measurements were more complicated due to an unstable temperature in the sample. Nevertheless, the thermal conductivity varies from 0.33 to 0.5 W/m.K from the ambient to 300°C. Both chars exhibit a low thermal conductivity (lower by 1 W/m.K) and so, heat insulating properties. These preliminary results are in the same order of magnitude as those found in the literature[5,15]. Slight differences between both char thermal conductivities may be explained by differences of expansion and porous media into both chars. To go further in the understanding, morphology analyses were performed to explain it. Based on these preliminary results, measurements will be further affined and then discussed in future work.

CONCLUSIONS AND PERSPECTIVES

In this study, the physical properties of carbonaceous products were examined in gaseous and condensed phases of materials exposed to fire. The focus was given to the morphology of soot (gaseous phase) for EVA and FR EVA and chars (condensed phase) for intumescent coatings. The abundance of soot in the gaseous phase is evidenced for EVA formulations. It is also evidenced that for the FR EVA/ATH system, soot formation is inhibited. The preliminary results on soot morphology evidenced hydrocarbon combustion and the results were consistent with our previous work and with literature on soot from hydrocarbon combustion. The results are to be further affined with future TEM imaging of soot and chemical analyses of specimens.

Concerning condensed phase analyses, the preliminary results on the intumescent char indicated the possible existence of a mass-density autocorrelation for the description of the inner structure. Therefore, the fractal analysis of char morphology is promising for future analyses and correlations to thermal properties, because it can reduce the complex morphology to simpler mathematical descriptions. The investigations of correlations between the morphology and thermal conductivities are in the perspectives.

REFERENCES

[1] Rothermel, R. C. (1972). A mathematical model for predicting fire spread in wildland fuels.
[2] Lyon, R. E. (1998). Pyrolysis kinetics of char forming polymers. Polymer Degradation and Stability, 61(2), 201-210.

[3] Lyon, R. E. (2000). Heat release kinetics. Fire and Materials, 24(4), 179-186.

[4] Sacadura, J.F. (2005). Radiative heat transfer in fire safety science, Journal of Quantitative Spectroscopy and Radiative Transfer, 93 (1–3), pp.5-24.

[5] Staggs, J.E.J. (2010). Thermal conductivity estimates of intumescent chars by direct numerical simulation, Fire Safety Journal, 45(4), pp.228-237.

[6] Girardin, B., Fontaine, G., Duquesne, S., Försth, M., & Bourbigot, S. (2015). Characterization of Thermo-Physical Properties of EVA/ATH: Application to Gasification Experiments and Pyrolysis Modeling. Materials, 8(11), 7837-7863.

[7] Ngohang, F. E., Fontaine, G., Gay, L., & Bourbigot, S. (2015). Smoke composition using MLC/FTIR/ELPI: Application to flame retarded ethylene vinyl acetate. Polymer Degradation and Stability, 115, 89-109.

[8] Carpentier, F., Bourbigot, S., Le Bras, M., Delobel, R., & Foulon, M. (2000). Charring of fire retarded ethylene vinyl acetate copolymer—magnesium hydroxide/zinc borate formulations. Polymer Degradation and Stability, 69(1), 83-92.

[9] Siat, C., Le Bras, M., & Bourbigot, S. (1998). Combustion behaviour of ethylene vinyl acetate copolymer-based intumescent formulations using oxygen consumption calorimetry. Fire and materials, 22(3), 119-128.

[10] Okyay, G., Héripré, E., Reiss, T., Haghi-Ashtiani, P., Auger, T., & Enguehard, F. (2016). Soot aggregate complex morphology: 3D geometry reconstruction by SEM tomography applied on soot issued from propane combustion. Journal of Aerosol Science, 93, 63-79.

[11] Okyay, G. (2016). Impact of the morphology of soot aggregates on their radiative properties and the subsequent radiative heat transfer through sooty gaseous mixtures (PhD dissertation, Université Paris Saclay, CentraleSupélec, France) – www.theses.fr/2016SACLC031

[12] Schneider, C. A., Rasband, W. S., & Eliceiri, K. W. (2012). NIH Image to ImageJ: 25 years of image analysis. Nature methods, 9(7), 671-675.

[13] Muller, M., Bourbigot, S., Duquesne, S., Klein, R., Giannini, G., Lindsay, C., & Vlassenbroeck, J. (2013). Investigation of the synergy in intumescent polyurethane by 3D computed tomography. Polymer degradation and stability, 98(9), 1638-1647.

[14] Jimenez, M., Duquesne, S., & Bourbigot, S. (2009). Kinetic analysis of the thermal degradation of an epoxy-based intumescent coating. Polymer Degradation and Stability, 94(3), 404-409.

[15] Staggs, J. E. J. (2011). Numerical characterization of the thermal performance of static porous insulation layers on steel substrates in furnace tests. Journal of Fire Sciences, 29 (2), 177-192.

[16] Gardelle, B., Duquesne, S., Vandereecken, P., & Bourbigot, S. (2013). Characterization of the carbonization process of expandable graphite/silicone formulations in a simulated fire. Polymer degradation and stability, 98(5), 1052-1063.

[17] Limodin, N., Rougelot, T., & Hauss, G. ISIS4D – In Situ Innovative Set-Ups under X-ray microtomography – http://isis4d.univ-lille1.fr/

[18] Ngohang, F. E., Fontaine, G., Gay, L., & Bourbigot, S. (2014). Revisited investigation of fire behavior of ethylene vinyl acetate/aluminum trihydroxide using a combination of mass loss cone, Fourier transform infrared spectroscopy and electrical low pressure impactor. Polymer Degradation and Stability, 106, 26-35.